

Accurate gradient computations at interfaces using finite element methods

Fangfang Qin ^{*} Zhaohui Wang[†] Zhijie Ma[‡] Zhilin Li^{§¶}

November 8, 2021

Abstract

New finite element methods are proposed for elliptic interface problems in one and two dimensions. The main motivation is not only to get an accurate solution but also an accurate first order derivative at the interface (from each side). The key in 1D is to use the idea from [24]. For 2D interface problems, the idea is to introduce a small tube near the interface and introduce the gradient as part of unknowns, which is similar to a mixed finite element method, except only at the interface. Thus the computational cost is just slightly higher than the standard finite element method. We present rigorous one dimensional analysis, which show second order convergence order for both of the solution and the gradient in 1D. For two dimensional problems, we present numerical results and observe second order convergence for the solution, and super-convergence for the gradient at the interface.

Keywords: elliptic interface problems, gradient/flux computation, IFEM, mixed FE formulation, computational tube.

AMS Subject Classification 2000: 65M06, 65M85.

1 Introduction

In this paper, we consider the following interface problems

$$-\nabla \cdot (\beta(\mathbf{x})\nabla u(\mathbf{x})) + q(\mathbf{x})u(\mathbf{x}) = f(\mathbf{x}), \quad \mathbf{x} \in \Omega \setminus \Gamma, \quad (1.1)$$

in one and two dimensions. We assume that there is a closed interface Γ in the solution domain across which the coefficient β has a finite jump (discontinuity)

$$\beta(\mathbf{x}) = \begin{cases} \beta_1 & \text{if } \mathbf{x} \in \Omega_1, \\ \beta_2 & \text{if } \mathbf{x} \in \Omega_2. \end{cases} \quad (1.2)$$

^{*}Jiangsu Key Laboratory for NSLSCS, School of Mathematical Sciences, Nanjing Normal University, Nanjing 210023, China

[†]Department of Mathematics, North Carolina State University, Raleigh, NC 27695

[‡]China Institute of Water Resource and Hydropower Research (IWHR), Beijing, China

[§]Department of Mathematics, North Carolina State University, Raleigh, NC 27695, USA and Nanjing Normal University. zhilin@math.ncsu.edu

[¶]Corresponding author.

Because of the discontinuity, the natural jump condition should be satisfied, that is, both of the solution and the flux should be continuous across the interface Γ

$$[u]_{\Gamma} = 0, \quad \left[\beta \frac{\partial u}{\partial n} \right]_{\Gamma} = 0, \quad (1.3)$$

where the jump at a point $\mathbf{X} = (X, Y)$ on the interface Γ is defined as

$$\left[\beta \frac{\partial u}{\partial n} \right]_{\mathbf{X}} = \lim_{\mathbf{x} \rightarrow \mathbf{X}, \mathbf{x} \in \Omega_2} \beta(\mathbf{x}) \frac{\partial u(\mathbf{x})}{\partial n} - \lim_{\mathbf{x} \rightarrow \mathbf{X}, \mathbf{x} \in \Omega_1} \beta(\mathbf{x}) \frac{\partial u(\mathbf{x})}{\partial n},$$

and $u_n = \mathbf{n} \cdot \nabla u = \frac{\partial u}{\partial n}$ is the normal derivative of solution $u(\mathbf{X})$, and \mathbf{n} is the unit normal direction pointing to Ω_2 side, see Fig. 1 for an illustration. Since a finite element discretization is used, we assume that $f(\mathbf{x}) \in L^2(\Omega_i)$, $q(\mathbf{x}) \in L^\infty(\Omega_i)$ excluding Γ . For the regularity requirement of the problem, we also assume that $\beta(\mathbf{x}) \geq \beta_0 > 0$ and $q(\mathbf{x}) \geq 0$; $\Gamma \in C^1$. From these assumptions, we know that the solution $u(\mathbf{x}) \in H^2(\Omega_i)$ for $i = 1, 2$.

There are many applications of such an interface problem, see for example, [17, 21, 28] and the references therein. Many numerical methods have been developed for solving such an important problem. For the elliptic interface problem (1.1)-(1.3), the solution has a low global regularity. Thus, a direct conforming finite element method based on polynomial basis functions over a mesh likely works poorly if the mesh is not aligned along the interface since the FE solution will be a smooth piece in an element and can not capture the discontinuity in the directive at the interface. Nevertheless, it is reasonable to assume that the solution is piecewise smooth excluding the interface. For example, if the coefficient is a piecewise constant in each sub-domain, then the solution in each sub-domain is an analytic function in the interior, but has jump in the normal derivative of the solution across the interface from the PDE limiting theory [14]. The gradient used in this paper is defined as the *limiting gradient* from each side of the interface.

Naturally, finite element methods can be and have been applied to solve interface problems. It is well known that a second order accurate approximation to the solution of an interface problem

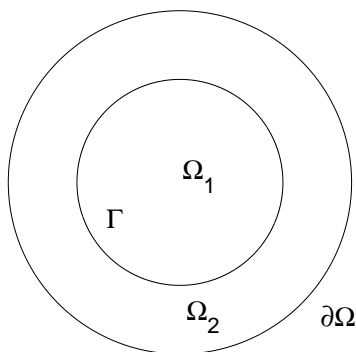


Figure 1: A diagram of domain Ω_1 , Ω_2 , an interface Γ , and the boundary $\partial\Omega$.

can be generated by the Galerkin finite element method with the standard linear basis functions if the triangulation is aligned with the interface, that is, a body fitted mesh is used, see for example, [3, 4, 7, 25]. Other state of art methods include the IGA-FEM, or DPG, a discontinuous Petrov-Galerkin finite element method [6]. Some kind of posterior techniques or at least quadratic elements are needed in order to get second order accurate gradient from each side of the interface. The cost in the mesh generation coupled with unstructured linear solver makes the body-fitted mesh approach less competitive.

Alternatively, we can use a structured mesh (non-body fitted) to solve such an interface problem. There are also quite a few finite element methods using Cartesian meshes. The immersed finite element method (IFEM) was developed for 1D and 2D interface problems in [16] and [18], respectively. Since then, many IFEM methods and analysis have appeared in the literature, see for example, [9, 12], with applications in [20, 26]. Often they provide second order accurate solution in L^2 norm but only first order accurate flux.

Nevertheless, in many applications the primary interest is focused on flux values at interfaces in addition to solutions of governing differential equations, see for example, [8, 10, 24]. Most of numerical methods for interface problems based on structure meshes are between first and second order accurate for the solution but the accuracy for the gradient is usually one order lower. Note that the gradient recovering techniques for examples, [23, 27], hardly work for structured meshes because of the arbitrariness of the interface and the underlying mesh. The mixed finite element approach and a few other methods that can find accurate solutions and gradients simultaneously in the entire domain are often lead to saddle problems and are computationally expensive which are not ideal choices if we are only interested in an accurate gradient near an interface or a boundary. In this paper, we develop two new finite element methods, one is in 1D, the other one is 2D, for obtaining accurate approximations of the flux values at interfaces.

The rest of the paper is organized as follows. In Section 2, we explain the one dimensional algorithm and provide the theoretical analysis. We explain how to construct approximations to the flux values at the left and the right of the interface, and approximations to the flux values at the boundary of the domain. The numerical algorithm for two dimensional problems is explained in Section 3 along with some numerical experiments. We conclude and acknowledge in Section 4.

2 One-dimensional algorithm and analysis

The one dimensional model problem has the following form,

$$\begin{aligned} -\left(\beta(x)u'(x)\right)' + q(x)u(x) &= f(x), \\ u(0) = 0, \quad u(1) &= 0, \end{aligned} \tag{2.1}$$

where $0 < x < 1$, β is a piecewise constant and have a finite jump at an interface $0 < \alpha < 1$, and homogenous boundary condition for simplicity of the discussion. Across the interface, the natural

jump conditions are:

$$[u]_\alpha = 0, \quad [\beta u'(x)]_\alpha = 0. \quad (2.2)$$

We define the standard bilinear form,

$$a(u, v) = \int_0^1 \left(\beta(x) u'(x) v'(x) + q(x) u(x) v(x) \right) dx, \quad \forall u(x), v(x) \in H_0^1(0, 1),$$

where $H_0^1(0, 1)$ is the Sobolev space [1, 5, 22].

$$H_0^1(0, 1) = \{v(x) \in H^1(0, 1) \text{ and } v(0) = v(1) = 0\}.$$

The solution of the differential equation $u(x) \in H_0^1(0, 1)$ is also the solution of the following variational problem:

$$a(u, v) = (f, v) = \int_0^1 f(x) v(x) dx, \quad \forall v(x) \in H_0^1(0, 1). \quad (2.3)$$

Integration by parts over the separated intervals $(0, \alpha)$ and $(\alpha, 1)$ yields,

$$0 = \int_0^\alpha \left\{ -(\beta u')' + qu - f \right\} v dx + \beta_1 u_x^- v^- + \int_\alpha^1 \left\{ -(\beta u')' + qu - f \right\} v dx - \beta_2 u_x^+ v^+.$$

The superscripts $-$ and $+$ indicate the limiting value as x approaches α from the left and right, respectively, and $u_x = u'$. Recall that $v^- = v^+$ for any v in H_0^1 , it follows that the differential equation holds in each interval and that

$$[u] = u^+ - u^- = 0, \quad [\beta u_x] = \beta^+ u_x^+ - \beta^- u_x^- = 0,$$

where we have dropped the subscript α in the jumps for simplicity. These relations are the same as in (2.1), which indicates that the discontinuity in the coefficient $\beta(x)$ does not cause any additional difficulty for the theoretical analysis of the finite element method. The weak solution will satisfy the jump conditions (2.2).

2.1 The immersed finite element method in 1D

Now we briefly explain the immersed finite element method (IFEM) in 1D introduced in [16]. As in the IFEM, we use a uniform grid, i.e., $x_i = ih, i = 0, 1, \dots, n$, and assume that $\alpha \in (x_j, x_{j+1})$. Since it is one dimensional problem, we use β^+ for β_2 , β^- for β_1 and so on.

If the interface does not cut an interval (x_i, x_{i+1}) , then we use the standard piecewise linear basis function, i.e., the hat function $\phi_i(x)$, $i = 1, 2, \dots$ if $i \neq j$ and $i \neq j + 1$. For x_j and x_{j+1} , the associated piecewise linear basis functions $\phi_j(x)$, $\phi_{j+1}(x)$ are modified. For example, $\phi_j(x)$ is defined as a piecewise linear function that satisfies

$$\varphi_j(x_j) = 1, \quad \varphi_j(x_i) = 0, \quad [\varphi_j] = 0, \quad [\beta \varphi_j'] = 0.$$

It has been derived in [17] that

$$\varphi_j(x) = \begin{cases} 0, & 0 \leq x < x_{j-1}, \\ \frac{x-x_{j-1}}{h}, & x_{j-1} \leq x < x_j, \\ \frac{x_j-x}{D} + 1, & x_j \leq x < \alpha, \\ \frac{\rho(x_{j+1}-x)}{D}, & \alpha \leq x < x_{j+1}, \\ 0, & x_{j+1} \leq x \leq 1, \end{cases}$$

where

$$\rho = \frac{\beta_1}{\beta_2}, \quad D = h - \frac{\beta_2 - \beta_1}{\beta_2} (x_{j+1} - \alpha),$$

and

$$\varphi_{j+1}(x) = \begin{cases} 0, & 0 \leq x < x_j, \\ \frac{x-x_j}{D}, & x_j \leq x < \alpha, \\ \frac{\rho(x-x_{j+1})}{D} + 1, & \alpha \leq x < x_{j+1}, \\ \frac{x_{j+2}-x}{h}, & x_{j+1} \leq x < x_{j+2}, \\ 0, & x_{j+2} \leq x \leq 1. \end{cases}$$

Let $V_{h,(0,1)} \triangleq \text{Span} \{\varphi_i\}_{i=1}^{n-1}$ be the immersed finite element space for approximating u . We propose the following bilinear form for problem (2.1): find $u_h \in V_{h,(0,1)} \subset H_0^1(0,1)$ such that

$$a(u_h, v_h) = (f, v_h), \quad \forall v_h \in V_{h,(0,1)}, \quad (2.4)$$

2.2 Error analysis for 1D IFEM

Some error analysis of 1D IFEM has been given in [16,17]. Here we provide somewhat different and more traditional analysis. As usual, we study the approximation property of the IFE space $V_{h,(0,1)}$ so that we can bound the error of the finite element solution using that of the interpolation function.

Assuming that $x_j \leq \alpha < x_{j+1}$, we define the interpolation operator $\pi_h : H_0^1(0,1) \rightarrow V_{h,(0,1)}$ as follows:

$$\pi_h u(x) = \begin{cases} \frac{x_{i+1}-x}{h} u(x_i) + \frac{x-x_i}{h} u(x_{i+1}), & x_i < x < x_{i+1}, \quad i \neq j, \\ \kappa(x-x_j) + u(x_j), & x_j < x \leq \alpha, \\ \kappa \frac{\beta_1}{\beta_2} (x-x_{j+1}) + u(x_{j+1}), & \alpha \leq x < x_{j+1}, \end{cases} \quad (2.5)$$

where

$$\kappa = \frac{\beta_2 (u(x_{j+1}) - u(x_j))}{\beta_2 (\alpha - x_j) - \beta_1 (\alpha - x_{j+1})}.$$

It is easy to verify that $\pi_h u(x_i) = u(x_i)$, $i = 0, 1, \dots, n$, $[\pi_h u] = 0$, and $[\beta \pi_h u'] = 0$.

Now we pay attention to the estimation of $\|u(x) - \pi_h u(x)\|_0$. Here, we define $E_i = [x_i, x_{i+1}]$, $i \neq j$ and $I = [x_j, x_{j+1}]$. For a regular element, we use the classical finite element method to estimate the error.

$$\|u - \pi_h u\|_{1,E_i} \leq ch \|u\|_{2,E_i}. \quad (2.6)$$

We are going to focus on the error analysis for the element which contains the interface. We first define

$$\tilde{H}^2(0,1) = \{v \in H_0^1(0,1), v \in H^2(0,\alpha), v \in H^2(\alpha,1)\}.$$

equipped with the norm and the semi-norm,

$$\|u\|_{\tilde{H}^2(0,1)}^2 \triangleq \|u\|_{H^2(0,\alpha)}^2 + \|u\|_{H^2(\alpha,1)}^2$$

and

$$|u|_{\tilde{H}^2(0,1)}^2 \triangleq |u|_{H^2(0,\alpha)}^2 + |u|_{H^2(\alpha,1)}^2.$$

Then we have the following error estimate for the derivative approximation, $\kappa \sim u_x^-$ from left.

Lemma 2.1. *If $u(x)$ is the solution of (2.1), the following inequality holds:*

$$\begin{aligned} |u_x^-(\alpha) - \kappa| &\leq ch^{\frac{1}{2}} \|u\|_{2,I}, \\ |u_x^+(\alpha) - \kappa\rho| &\leq ch^{\frac{1}{2}} \|u\|_{2,I}. \end{aligned} \tag{2.7}$$

Proof. Using the Taylor expansion at α and the jump conditions (i.e., (2.2)), we have

$$\begin{aligned} |u_x^-(\alpha) - \kappa| &= \left| u_x^-(\alpha) - \frac{\beta_2(u(x_{j+1}) - u(x_j))}{\beta_2(\alpha - x_j) - \beta_1(\alpha - x_{j+1})} \right| \\ &= \left| u_x^-(\alpha) - \frac{\beta_2 \left\{ u^+(\alpha) + u_x^+(\alpha)(x_{j+1} - \alpha) + \int_{\alpha}^{x_{j+1}} u''(t)(x_{j+1} - t) dt \right\}}{\beta_2(\alpha - x_j) - \beta_1(\alpha - x_{j+1})} \right. \\ &\quad \left. - \frac{u^-(\alpha) + u_x^-(\alpha)(x_j - \alpha) + \int_{\alpha}^{x_j} u''(t)(x_j - t) dt}{\beta_2(\alpha - x_j) - \beta_1(\alpha - x_{j+1})} \right| \\ &= \left| \frac{\beta_2 \left[\int_{\alpha}^{x_{j+1}} u''(t)(x_{j+1} - t) dt - \int_{\alpha}^{x_j} u''(t)(x_j - t) dt \right]}{\beta_2(\alpha - x_j) - \beta_1(\alpha - x_{j+1})} \right| \\ &\leq ch^{\frac{1}{2}} \|u\|_{2,I}, \quad (\text{Cauchy - Schwarz Inequality}) \end{aligned}$$

where c is a positive constant depending only on the coefficients $\beta, q(x)$. This completes the proof of the lemma. \square

The lemma gives rough estimates of the first order derivative of the interpolation function from each side of the interface with an $O(\sqrt{h})$ convergence order compared with that $O(h)$ in the $H^1(0,1)$ of the interpolation function. Later on, we will explain our method to get second order accurate derivative from each side of the interface.

In a similar way, we can prove that

$$|u_x^+(\alpha) - \kappa\rho| \leq ch^{\frac{1}{2}} \|u\|_{2,I}.$$

2.3 Convergence analysis of 1D IFEM

Although some error analysis is given in [16], below we provide some different, more traditional finite element analysis with some results that are useful for accurate gradient computations at the interface. First we prove the following theorem on the accuracy of the interpolating function $\pi_h u$.

Theorem 2.2. *If $u(x)$ is the solution of (2.1), and $\pi_h u(x)$ is the interpolation function defined in (2.5), then*

$$\|u - \pi_h u\|_{1,I} \leq ch \|u\|_{2,I}, \quad (2.8)$$

where c is a positive constant depending on the interface location, the coefficients β , and $q(x)$.

Proof. Proof of theorem If $x_j \leq x \leq \alpha$, then using the Taylor expansion, we have

$$\begin{aligned} u(x) &= u(x_j) + u'(x_j)(x - x_j) + \int_{x_j}^x u''(t)(x - t) dt \\ &= u(x_j) + \left[u_x^-(\alpha) + \int_{\alpha}^{x_j} u''(x) dx \right] (x - x_j) + \int_{x_j}^x u''(t)(x - t) dt \\ &= u(x_j) + u_x^-(\alpha)(x - x_j) + \int_{\alpha}^{x_j} u''(x) dx (x - x_j) + \int_{x_j}^x u''(t)(x - t) dt. \end{aligned}$$

By (2.7) and the Cauchy-Schwartz inequality, we get

$$\begin{aligned} |u(x) - \pi_h u(x)| &= \left| (u_x^-(\alpha) - k)(x - x_j) + \int_{\alpha}^{x_j} u''(x) dx (x - x_j) + \int_{x_j}^x u''(t)(x - t) dt \right| \\ &\leq ch^{\frac{3}{2}} \|u\|_{2,I}, \end{aligned}$$

and furthermore

$$\begin{aligned} |(u(x) - \pi_h u(x))'| &= \left| u_x^-(\alpha) - k + \int_{\alpha}^{x_j} u''(x) dx + \int_{x_j}^x u''(t) dt \right| \\ &\leq ch^{\frac{1}{2}} \|u\|_{2,I}. \end{aligned}$$

If $\alpha \leq x \leq x_{j+1}$, the proof is similar. Thus we also have,

$$|u(x) - \pi_h u(x)| \leq ch^{\frac{3}{2}} \|u\|_{2,I}, \quad |(u(x) - \pi_h u(x))'| \leq ch^{\frac{1}{2}} \|u\|_{2,I}.$$

We proceed with the remaining proof below

$$\begin{aligned} \|u(x) - \pi_h u(x)\|_{0,I} &= \left(\int_{x_j}^{\alpha} (u(x) - \pi_h u(x))^2 dx + \int_{\alpha}^{x_{j+1}} (u(x) - \pi_h u(x))^2 dx \right)^{\frac{1}{2}} \\ &\leq c \left(\int_{x_j}^{\alpha} h^3 \|u\|_{2,I}^2 dx + \int_{\alpha}^{x_{j+1}} h^3 \|u\|_{2,I}^2 dx \right)^{\frac{1}{2}} \\ &\leq ch^2 \|u\|_{2,I}, \end{aligned}$$

in L^2 and we continue to H^1 ,

$$\begin{aligned} |u(x) - \pi_h u(x)|_{1,I} &= \left(\int_{x_j}^{\alpha} [(u(x) - \pi_h u(x))']^2 dx + \int_{\alpha}^{x_{j+1}} [(u(x) - \pi_h u(x))']^2 dx \right)^{\frac{1}{2}} \\ &\leq ch \|u\|_{2,I}. \end{aligned}$$

Combining all above to get,

$$\begin{aligned} \|u(x) - \pi_h u(x)\|_{1,I} &= \left(\|u(x) - \pi_h u(x)\|_{0,I}^2 + |u(x) - \pi_h u(x)|_{1,I}^2 \right)^{\frac{1}{2}} \\ &\leq ch \|u\|_{2,I}, \end{aligned}$$

which completes the proof. \square

The following theorem states that the IFEM in 1D provides optimal convergence as that the FEM for regular problems.

Theorem 2.3. *If $u(x)$ is the solution of (2.1), and $\pi_h u(x)$ is the interpolating function defined in (2.5), then*

$$\|u - \pi_h u\|_1 \leq ch \|u\|_2, \quad (2.9)$$

Proof. We would using (2.6) and (2.8) to get

$$\begin{aligned} \|u(x) - \pi_h u(x)\|_1 &= \left(\int_0^1 (u(x) - \pi_h u(x))^2 + \left((u(x) - \pi_h u(x))' \right)^2 dx \right)^{\frac{1}{2}} \\ &= \left(\sum_{E_i} \|u - \pi_h u\|_{1,E_i}^2 + \|u - \pi_h u\|_{1,I}^2 \right)^{\frac{1}{2}} \\ &\leq \left(\sum_{E_i} ch^2 \|u\|_{2,E_i}^2 + ch^2 \|u\|_{2,I}^2 \right)^{\frac{1}{2}} \\ &\leq ch \left(\sum_{E_i} \|u\|_{2,E_i}^2 + \|u\|_{2,I}^2 \right)^{\frac{1}{2}} \\ &\leq ch \|u\|_2. \end{aligned}$$

This completes the proof of the theorem. \square

2.4 An accurate flux computation at the left of the interface

In this sub-section, we explain how to get an accurate flux or first order derivative of the solution at the interface from the left side of the interface. The method is based on the approach proposed in [24] for flux computations at boundaries. The method is based on the use of the Galerkin solution of the problem and it is different from other posterior error analysis.

We define the following Γ_α^-

$$\Gamma_\alpha^- \triangleq \frac{1}{\alpha} \{(\beta u_h', 1)_{(0,\alpha)} + (qu_h - f, x)_{(0,\alpha)}\}, \quad (2.10)$$

as an approximation to the exact flux $\beta_1 u_x^-(\alpha)$. Below we show that this is a second order approximation which improves the accuracy of the flux by one order compared the estimate in (2.9).

Theorem 2.4. *If $u(x)$ is the solution of (2.1), $u_h(x)$ is the Galerkin approximation of the solution of $u(x)$, Γ_α^- is as defined above, then*

$$|\Gamma_\alpha^- - \beta_1 u_x^-(\alpha)| \leq ch^2 \|u\|_2. \quad (2.11)$$

Proof. We define $Y \in V_h$ as a function that satisfied $Y(0) = 0$ and

$$\left(\beta Y', v_h'\right)_{(0,\alpha)} + (qY - f, v_h)_{(0,\alpha)} = \beta_1 u_x^-(\alpha) v_h(\alpha), \quad \forall v_h \in V_h, \text{ and } v_h(0) = 0. \quad (2.12)$$

Subtracting (2.10) with $v_h = x/\alpha$ from (2.12), we have

$$\begin{aligned} |\Gamma_\alpha^- - \beta_1 u_x^-(\alpha)| &= \frac{1}{\alpha} \left| \left(\beta (u_h - Y)', 1\right)_{(0,\alpha)} + (q(u_h - Y), x)_{(0,\alpha)} \right| \\ &\leq c \{ \|u_h - Y\|_0 + |(u_h - Y)(\alpha)| \}. \end{aligned}$$

From (2.4) and (2.12) we can see that

$$\left(\beta (u_h - Y)', v_h'\right)_{(0,\alpha)} + (q(u_h - Y), v_h)_{(0,\alpha)} = 0, \quad \forall v_h \in V_{h,(0,\alpha)}; \quad (2.13)$$

Set $w = u_h - Y$, and $v_h = w - xw(\alpha)$, we get the following equation

$$\left(\beta w', w'\right)_{(0,\alpha)} + (qw, w)_{(0,\alpha)} = \left(\beta w', w(\alpha)\right)_{(0,\alpha)} + (qw, xw(\alpha))_{(0,\alpha)},$$

and thus we have

$$\|w\|_1 \leq c \{ \|w\|_0 + |w(\alpha)| \}. \quad (2.14)$$

Next we construct the following auxiliary problem. Let $\varphi \in H^2(0, \alpha) \cap \tilde{H}^1(0, \alpha)$ be the solution of the following

$$\begin{cases} L^* \varphi = -w, & w \in (0, \alpha), \\ \varphi(0) = \varphi(\alpha) = 0. \end{cases}$$

We also assume that

$$\|\varphi\|_2 \leq c \|w\|_0.$$

Then, for an appropriately chosen $\pi\varphi \in V_{h,(0,\alpha)}$, we proceed to get the following,

$$\begin{aligned}
(w, w)_{(0,\alpha)} &= \left| -(w, L^*\varphi)_{(0,\alpha)} \right| = \left| \left(w, \left(\beta\varphi' \right)' - q\varphi \right)_{(0,\alpha)} \right| \\
&= \left| - \left(\beta w', \varphi' \right)_{(0,\alpha)} - (qw, \varphi)_{(0,\alpha)} + \left(\beta^- \varphi' w \right) (\alpha) \right| \\
&\leq \left| \left(\beta w', \varphi' - (\pi\varphi)' \right)_{(0,\alpha)} \right| + \left| (qw, \varphi - x)_{(0,\alpha)} \right| + \left| \left(\beta\varphi' w \right) (\alpha) \right| \\
&\leq c \left\{ \|w\|_1 \|\varphi - \pi\varphi\|_1 + \left| \varphi' (\alpha) \right| |w(\alpha)| \right\} \\
&\leq c \{ h \|w\|_1 \|\varphi\|_2 + \|w\|_0 |w(\alpha)| \} \\
&\leq c \|w\|_0 \{ h \|w\|_1 + |w(\alpha)| \}.
\end{aligned}$$

The above yields,

$$\|w\|_0 \leq c \{ h \|w\|_1 + |w(\alpha)| \}. \quad (2.15)$$

For h sufficiently small (2.14) and (2.15) imply that

$$\|w\|_0 \leq c |w(\alpha)|, \quad (2.16)$$

where c is a positive constant depending only on the coefficients $\beta, q(x)$.

We now derive an estimate of $|w(\alpha)|$, using the new auxiliary problem

$$\begin{cases} L^*\xi = 0, & \xi \in (0, \alpha), \\ \xi(0) = 0, & \beta_1(\alpha) \xi'(\alpha) = 1. \end{cases}$$

Let $\eta = u - Y$, then we can get

$$\left(\beta\eta', v_h \right)_{(0,\alpha)} + (q\eta, v_h)_{(0,\alpha)} = 0, \quad \forall v_h \in V_h \text{ such that } v_h(0) = 0. \quad (2.17)$$

Furthermore, using

$$\begin{aligned}
0 &= -(\eta, L^*\xi)_{(0,\alpha)} = - \left(\eta, - \left(\beta\xi' \right)' + q\xi \right)_{(0,\alpha)} \\
&= \left(\eta, \left(\beta\xi' \right)' - q\xi \right)_{(0,\alpha)} \\
&= \left(-\beta\eta', \xi' \right)_{(0,\alpha)} + (-q\eta, \xi)_{(0,\alpha)} + \eta(\alpha),
\end{aligned}$$

we have

$$\begin{aligned}
|\eta(\alpha)| &= \left| \left(\beta\eta', \xi' \right)_{(0,\alpha)} + (q\eta, \xi)_{(0,\alpha)} \right| \\
&\leq c \|\eta\|_1 \|\xi - x\|_1 \\
&\leq ch \|\eta\|_1 \\
&\leq ch^2 \|u\|_2.
\end{aligned}$$

Finally, we get

$$\begin{aligned} |\Gamma_\alpha^- - \beta_1 u_x^-(\alpha)| &\leq c |(u_h - Y)(\alpha)| \\ &\leq c \{|(u - u_h)(\alpha)| + |(u - Y)(\alpha)|\} \\ &\leq ch^2 \|u\|_2. \end{aligned}$$

This completes the proof of the theorem. \square

Approximation of flux from the right side of the interface

In the similar way, we can get the second order accurate flux, $-\beta^+ u_x^+$, from the right side of the interface

$$\Gamma_\alpha^+ \triangleq \frac{1}{1-\alpha} \{(\beta u_h', -1)_{(\alpha,1)} + (qu_h - f, 1-x)_{(\alpha,1)}\}.$$

We also have the following error bound.

$$|\Gamma_\alpha^+ + \beta^+ u_x^+(\alpha)| \leq ch^2 \|u\|_2.$$

Approximation of fluxes at the boundary

The approach for accurate flux computations at the interface can be applied to the flux computation from the left and right boundaries as expressed below. We define approximations Γ_0 and Γ_1 to the fluxes, $\beta_1 u'(0)$ and $\beta_2 u'(1)$ respectively:

$$\Gamma_0 \triangleq (\beta u_h', -1) + (qu_h - f, 1-x),$$

$$\Gamma_1 \triangleq (\beta u_h', 1) + (qu_h - f, x).$$

Then Γ_0 and Γ_1 are second order approximations to the flux from the left and right boundaries as stated in the following theorem. We skip the proof since it is similar to that for the flux from the left side of the interface.

Theorem 2.5. *If $u(x)$ is the solution of (2.1), $u_h(x)$ is the Galerkin approximation of the solution of $u(x)$, Γ_0 and Γ_1 are as defined above, then*

$$\left| \Gamma_0 + \beta_1 u'(0) \right| + \left| \Gamma_1 - \beta_2 u'(1) \right| \leq ch^2 \|u\|_2.$$

2.5 Numerical experiments in 1D

We present one example below that is taken from [17]. The exact solution is

$$u(x) = \begin{cases} x^4/\beta^-, & \text{if } 0 < x < \alpha, \\ x^4/\beta^+ + (1/\beta^- - 1/\beta^+)\alpha^4, & \text{if } \alpha < x < 1, \end{cases}$$

where $0 < \alpha < 1$ is an interface. The solution satisfies the ODE $-(\beta u')' = f(x)$ where $f(x) = -12x^2$. In this example, $q(x) = 0$ and $[u] = 0$ and $[\beta u'] = 0$, but $[u'] \neq 0$.

In Table 1, we show a grid refinement analysis for the proposed method with $\alpha = 1/3$, $\beta^- = 2$, $\beta^+ = 10$. Thus the interface α is not a nodal point. We measure the error for the solution $u(x)$ in the entire domain $(0, 1)$ in the second column using the strongest norm L^∞ norm. We estimate the convergence order using $p = \log(E_n/E_{2N})/\log 2$ in the third column. As usual, since the relative location between the underlying grid and the interface α is not fixed, the convergence order fluctuates. The average convergence order is 1.983. In the third column, we list the grid refinement analysis for $u_x^- = \lim_{x \rightarrow \alpha, x < \alpha} u'(x)$, that is, the first order derivative from the left side of the interface, we observe clear second order convergence as shown in the fifth column.

N	$\ u - u_h\ _{L^\infty}$	Order	$ u - u_h _{H^1}$	Order
16	3.395E-05		3.870E-03	
32	1.547E-05	1.134	7.980E-04	2.278
64	2.191E-06	2.820	1.562E-04	2.353
128	9.732E-07	1.171	3.892E-05	2.005
256	1.413E-07	2.784	8.475E-06	2.199
512	6.088E-08	1.215	2.263E-06	1.905
1024	8.900E-09	2.774	5.098E-07	2.150

Table 1: A grid refinement analysis of the proposed method with $\alpha = 1/3$, $\beta^- = 2$, $\beta^+ = 10$. The second column is the L^∞ error of the solution in the entire domain $(0, 1)$. The fourth column is the error in the first order derivative u_x^- , that is, from the left side of the interface. The average convergence order for the solution and u_x^- are 1.983 and 2.148, respectively.

3 The numerical method and experiments for the 2D interface problem

The results in the previous section are the optimal since both the solution and the flux (at the interface or boundaries) using a piecewise linear finite element space. However, it is still an open question how to apply the approach to 2D problems with a curved interface. In this section, we provide an alternative approach that is similar to a mixed finite element method but only in a small tube around the interface.

In this section, the elliptic interface problem is

$$-\nabla \cdot (\beta \nabla u(\mathbf{x})) + q(\mathbf{x})u(\mathbf{x}) = f(\mathbf{x}), \quad \mathbf{x} \in \Omega_i, \quad i = 1, 2, \quad (3.1)$$

where $q(\mathbf{x}) \in L^\infty(\Omega) \geq 0$, $\Omega = \Omega^- \cup \Omega^+$, $\beta(\mathbf{x})$ is a piecewise positive constant as in (1.2) and has a finite jump discontinuity across a closed interface $\Gamma \in C^1$ in the solution domain.

In our new method, we introduce a tube that contains the interface with a diameter 2ϵ as

$$\Omega_\epsilon = \{\mathbf{x} \in \Omega_1 \cup \Omega_2, \quad d(\mathbf{x}, \Gamma) \leq \epsilon\},$$

where $d(\mathbf{x}, \Gamma)$ is the distance between \mathbf{x} and the interface Γ . In the tube Ω_ϵ , we introduce the flux as a separate variable vector \mathbf{v} that can be considered as an augmented variable. Thus, in addition to the PDE (3.1) in the entire domain, we also have the following equations

$$\begin{aligned} -\beta \nabla u &= \mathbf{v}, \\ \nabla \cdot \mathbf{v} + qu &= f, \end{aligned} \quad \mathbf{x} \in \Omega_\epsilon.$$

Next we define the following functional spaces

$$\begin{aligned} H_0^1 &= \{ \phi \in H^1(\Omega), \quad \phi = 0 \text{ on } \partial\Omega \}, \\ W &= \{ w \in L^2(\Omega_\epsilon) \}, \\ L_g &= \{ \mathbf{g} \in (L^2(\Omega_\epsilon))^2 \}, \end{aligned}$$

assuming homogenous boundary condition along $\partial\Omega_2$.

We can easily get the following weak form for u (in the entire domain) and \mathbf{g} (in Ω_ϵ) below

$$(\beta_i \nabla u, \nabla \phi) + (qu, \phi) = (f, \phi) \text{ in } \Omega_i, \quad i = 1, 2, \quad (3.2)$$

$$-(\beta_i \nabla u, \mathbf{g}) = (\mathbf{v}, \mathbf{g}) \text{ in } \Omega_\epsilon \cap \Omega_i, \quad i = 1, 2, \quad (3.3)$$

$$(\nabla \cdot \mathbf{v}, w) + (qu, w) = (f, w) \quad \text{in } \Omega_\epsilon, \quad (3.4)$$

where the inner product is in the regular L^2 sense and those quantities ϕ , \mathbf{g} , and w are from the spaces defined above.

There are two intuitive reasonings behind the new algorithm. We know that the mixed formulation would improve the gradient computation. If we are only interested in the gradient from each side of the interface, then we just need to use a small tube for the computation. The second consideration is that if we set the flux $\mathbf{v} = \beta \nabla u$ along the interface as an unknown in addition to the solution u , and then discretize the whole system with high order discretization (second order in the manuscript), then we would expect the error for the unknown flux \mathbf{v} would have the same order of accuracy as for the discretization. In discretization, we use piecewise linear functions for ϕ and \mathbf{g} as usual, and piecewise constant functions for w . The new augmented method enlarged the system by (3.3) and (3.4). In terms of the stiffness matrix, an additional n_v number of columns are added to the stiffness matrix where n_v is the number of extra unknowns \mathbf{v} in the tube Ω_ϵ . As a result, the stiffness matrix becomes a rectangular matrix instead of a square matrix. We used the singular value decomposition (SVD) to solve the resultant rectangular system. Since \mathbf{v} has co-dimension one compared with that of u , the additional extra cost is negligible compared with that of the elliptic solver on the entire domain.

3.1 Numerical experiments in 2D

Let Ω_2 be a unit circle centered at $(0,0)$ with radius $R = 1$. In our numerical test, we take $q = 0$. Let Γ be an interface inside the unit circle with radius $R = 0.9$. The tube width is taken as $\epsilon = 3h$, that is three layers from each side of the interface. The exact solution is

$$u(x, y) = \sin x \cos y, \quad (3.5)$$

in the entire domain so that the solution is continuous, but the flux $\beta \nabla u$ is discontinuous for the test problem. The coefficient is taken as $\beta_1 = 100$ and $\beta_2 = 1$. The source terms and boundary

condition are determined accordingly. In Table 2, the L^2 norm errors of u , \mathbf{v} , and the H^1 norm error of u are reported. The $L^2(\Omega)$, $H^1(\Omega)$ are used for the solution u , that is, in the entire domain, while $L^2(\Gamma)$ is used for the flux along the interface.

The first column N is the mesh lines in the coordinates directions. The results indicate that the new augmented method worked as expected. The convergence rate is shown in Table 3.

N	L^2 error of u	H^1 error of u	L^2 error of \mathbf{v}
8	9.96e-3	5.67e-1	5.67e-1
16	2.48e-3	1.75e-1	1.75e-1
32	7.77e-4	4.14e-2	4.14e-2
64	1.81e-4	1.04e-2	1.04e-2
128	4.71e-5	5.95e-3	5.95e-3
256	1.15e-5	1.54e-3	1.54e-3
512	2.92e-6	3.80e-4	3.80e-4

Table 2: A grid refinement analysis of the proposed method. The H^1 norm of u is the same as the L^2 error of \mathbf{v} because the error in the gradient is dominated compared with that of u .

In Table 3, a comparison of the convergence order between the standard finite element method and the new augmented approach is presented. We observe that the new approach provides much better accuracy for the flux (gradient). Now we have super-convergence for the gradient. Super-convergence here is the result of the convergence that is faster than the original method. For the finite element method with the piecewise linear function space, it is well-known that the flux is first order accurate in the L^2 norm. In our manuscript, We proposed a method to reconstruct the flux at the interface and has shown that the reconstructed flux has second order convergence.

Quantity	u	u	\mathbf{v}
Norm	L^2	H^1	L^2
Order (standard FEM)	1.98	1.03	1.03
Order (new method)	1.94	1.72	1.72

Table 3: A comparison of the convergence order between the standard FEM and the new augmented approach.

Next, in Table 4 we present the results with different interface locations including the case that covers the entire domain ($r_i = 0$) so that we get the gradient in the entire domain as well, where r_i is the radius of the interface. Of course, the computational cost also increased. As we expected, we have second order convergence in the L^2 norm for the solution, and roughly 1.70 order for the flux (gradient). In this case, the accuracy of the gradient is improved by about 70 percent.

r_i	Order in L^2 of u	order in H^1
0.9	1.94	1.72
0.99	1.94	1.70
0	1.93	1.70

Table 4: A comparison of the convergence order for various location of the interface, where r_i is the radius of the interface.

Now we show the result with a non-zero $q(x, y)$. We use the same solution above with $q(x, y) = 1$. The source term is modified accordingly. In Table 5, we show the grid refinement analysis of the error in L^2 and H^1 norm. We observe the same behavior with the similar convergence orders. The average convergence orders are 1.92 for the L^2 norm, 1.71 for the H^1 norm, respectively. Note that, the L^2 norm of the error in \mathbf{v} is the same as the H^1 norm as explained earlier.

N	L^2 error of u	H^1 error of u
8	9.96e-3	5.67e-1
16	3.51e-3	2.61e-1
32	1.17e-4	6.54e-2
64	2.81e-4	1.66e-2
128	7.24e-5	9.13e-3
256	1.85e-5	2.31e-3
512	4.62e-6	5.79e-4

Table 5: A grid refinement analysis of the proposed method when $q(x, y) = 1$. The average convergence orders are 1.92 for the L^2 norm, 1.71 for the H^1 norm, respectively.

In the previous example, the solution is the same in the entire domain in spite of the flux is discontinuous. Below we present another example in which the solution is different in different domain. The outer boundary is $R = 2$.

$$u(x, y, t) = \begin{cases} (x^2 + y^2)^2 & \text{if } r > 1, \\ (x^2 + y^2) & \text{if } r \leq 1, \end{cases} \quad (3.6)$$

where $r = \sqrt{x^2 + y^2}$. The source term $f(x, y)$, and the Dirichlet boundary condition are determined from the true solution. In this example, the solution is continuous, that is, $[u] = 0$, but the flux jump is non-homogeneous.

We tested our new method with large jump ratios $\beta_2 : \beta_1 = 1000 : 1$ and $\beta_2 : \beta_1 = 1 : 1000$. In Table 6, we present the results with different widths of the tube including the case that covers the entire domain so that we get the gradient in the entire domain as well. As we expected, we have second order convergence in the L^2 norm for the solution, and roughly 1.54 order for the flux (gradient) as in the thin tube case. Compared with the standard finite element method, the accuracy of the computed gradient is improved by more than 50 percent. Note that the results are almost the same as the new gradient recovery technique using a posterior approach [11] in which

the rate of the recovered gradient is around 1.5. Note that, the convergence order for the gradient is about 1.54 which is lower than the previous case possibly due to the non-homogenous flux jump.

width (ϵ)	Order in L^2 of u	order in H^1
$3h$	1.96	1.53
$10h$	1.96	1.56
2 (entire domain)	1.96	1.56

Table 6: A comparison of the convergence order for various widths of the tube.

4 Conclusions

In this paper, we discussed two methods to enhance the accuracy of the computed flux at the interface for the elliptic interface problem. One is for one-dimensional problems in which we use a simple weak form to get second order accurate fluxes at the interface from each side. We also have rigorous analysis for the approach. The other one is an augmented approach for two dimensional interface problems. Numerical examples show that we get better than super-convergence (about $1.50 \sim 1.70$ order) for the computed fluxes at the interface from each side. For the two dimensional algorithm, the theoretical analysis is still an open challenge.

Acknowledgment

The authors would like to thank the following supports. F. Qin is partially supported by China NSF Grants 11691209, 11691210 and the NSF of Jiangsu Province, China (Grant No. BK20160880). Z. Ma is supported by China National Special Fund: 2012DFA60830, and Z. Li would is partially supported by the US NSF grant DMS-1522768, and China NSF grant 11371199 and 11471166.

References

- [1] R. Adams and J. Fournier. *Sobolev spaces. Second edition*, Pure and Applied Mathematics (Amsterdam), 140. Elsevier/Academic Press, Amsterdam, 2003.
- [2] N. An and H. Chen. A partially penalty immersed interface finite element method for anisotropic elliptic interface problems. *Numerical Methods for Partial Differential Equation*, 30: 1984–2028, 2014.
- [3] I. Babuška. The finite element method for elliptic equations with discontinuous coefficients. *Computing*, 5: 207–213, 1970.
- [4] J. Bramble and J. King. A finite element method for interface problems in domains with smooth boundaries and interfaces. *Advances in Computational Mathematics*, 6: 109–138, 1996.

- [5] S. Brenner and R. Scott. *The mathematical theory of finite element methods*, volume 15. Springer Science & Business Media, 2007.
- [6] C. Carstensen, D. Gallistlb, F. Hellwiga and L. Wegglera. Low-order dPG-FEM for an elliptic PDE. *Computers Mathematics with Applications*, 68(11): 1503–1512, 2014
- [7] Z. Chen and J. Zou. Finite element methods and their convergence for elliptic and parabolic interface problems. *Numerische Mathematik*, 79: 175–202, 1998.
- [8] S. Chou. An immersed linear finite element method with interface flux capturing recovery. *Discrete and Continuous Dynamical Systems Series B*, 17: 2343–2357, 2012.
- [9] S. Chou, D. Kwak, and K. Wee. Optimal convergence analysis of an immersed interface finite element method. *Advances in Computational Mathematics*, 33: 149–168, 2010.
- [10] J. Douglas, T. Dupont, and M. Wheeler. A Galerkin procedure for approximating the flux on the boundary for elliptic and parabolic boundary value problems. *RAIRO Model. Math. Anal. Numer.*, 8: 47–59, 1974.
- [11] H. Guo X. Yang. Gradient recovery for elliptic interface problem: II. Immersed finite element methods. arXiv:1608.00063, 2016.
- [12] X. He, T. Lin, and Y. Lin. Immersed finite element methods for elliptic interface problems with non-homogeneous jump conditions. *International Journal of Numerical Analysis and Modeling*, 8: 284–301, 2010.
- [13] H. Ji, J. Chen, and Z. Li. A new augmented immersed finite element method without using SVD interpolations. *Numerical Algorithms*, 71: 395–416, 2016.
- [14] J. Kevorkian. *Partial differential equations*, Wadsworth & Brooks/Cole, 1990.
- [15] D. Kwak, K. Wee, and K. Chang. An analysis of a broken P_1 -nonconforming finite element method for interface problems. *SIAM Journal on Numerical Analysis*, 48: 2117–2134, 2010.
- [16] Z. Li. The immersed interface method using a finite element formulation. *Applied Numerical Mathematics*, 27: 253–267, 1998.
- [17] Z. Li and K. Ito. *The immersed interface method: numerical solutions of PDEs involving interfaces and irregular domains*, volume 33. SIAM, 2006.
- [18] Z. Li, T. Lin, and X. Wu. New Cartesian grid methods for interface problems using the finite element formulation. *Numerische Mathematik*, 96: 61–98, 2003.
- [19] T. Lin, Y. Lin and X. Zhang. Partially penalized immersed finite element methods for elliptic interface problems. *SIAM Journal on Numerical Analysis*, 53: 1121–1144, 2015.

- [20] T. Lin and X. Zhang. Linear and bilinear immersed finite elements for planar elasticity interface problems. *Journal of Computational and Applied Mathematics*, 236: 4681–4699, 2012.
- [21] A. Sutton and R. Balluffi. *Interfaces in crystalline materials*. Clarendon Press, 1995.
- [22] L. Tartar. *An introduction to Sobolev spaces and interpolation spaces*. Lecture Notes of the Unione Matematica Italiana, 3. Springer, Berlin; UMI, Bologna, 2007.
- [23] L. Wahlbin. *Superconvergence in Galerkin finite element methods*, Lecture Notes in Mathematics, vol. 1605, Springer-Verlag, Berlin, 1995.
- [24] M. Wheeler. A Galerkin procedure for estimating the flux for two-point boundary value problems. *SIAM Journal on Numerical Analysis*, 11: 764–768, 1974.
- [25] J. Xu. Error estimates of the finite element method for the 2nd order elliptic equations with discontinuous coefficients. *Journal of Xiangtan University* , 1: 1–5, 1982.
- [26] X. Yang, B. Li, and Z. Li. The immersed interface method for elasticity problems with interface. *Dynamics of Continuous, Discrete and Impulsive Systems*, 10: 783–808, 2003.
- [27] Z. Zhang and A. Naga. A new finite element gradient recovery method: superconvergence property. *SIAM Journal on Scientific Computing*, 26: 1192–1213, 2005.
- [28] O. Zienkiewicz and R. Taylor. *The finite element method: solid mechanics*, volume 2. Butterworth-Heinemann, 2000.